JACS ARTICLES

Published on Web 03/12/2010

Hydroxyl-Rich β-Sheet Adhesion to the Gold Surface in Water by First-Principle Simulations

Arrigo Calzolari,[†,‡] Giancarlo Cicero,[§,⊥] Carlo Cavazzoni,[△] Rosa Di Felice,[†] Alessandra Catellani,[⊥] and Stefano Corni*[,†]

Centro S3, CNR-Istituto di Nanoscienze, Modena, Italy, Department of Material Science and Chemical Engineering, Politecnico of Torino, Torino, Italy, CNR-IMEM Institute of Materials for Electronics and Magnetisms, Parma, Italy, and CINECA, Interuniversity Computing Center, Bologna, Italy

Received November 25, 2009; E-mail: stefano.corni@unimore.it

Abstract: Proteins able to recognize inorganic surfaces are of paramount importance for living organisms. Mimicking nature, surface-recognizing proteins and peptides have also been man-made by combinatorial biochemistry. However, to date the recognition mechanisms remain elusive, and the underlying physicochemical principles are still unknown. Selectivity of gold-binding peptides (cysteine-free and rich in hydroxyl amino acids) is particularly puzzling, since the most relevant gold surface, Au(111), is known to be chemically inert and atomically flat. Using atomistic first-principle simulations we show that weak chemical interactions of dative-bond character confer to a prototype secondary structure (an antiparallel β-sheet made of hydroxyl amino acids) and its hydration layer the capability of discriminating among gold surface sites. Our results highlight the unexpected role of hydration water in this process, suggesting that hydrophilic amino acids and their hydration shell cooperate to contribute to protein−gold surface recognition.

Introduction

Proteins able to recognize inorganic surfaces are of paramount importance for the growth of natural materials.[1,2] Mimicking nature, surface-recognizing proteins and peptides have been man-made by combinatorial biotechniques.[3−5] Their potential for nanotechnology and biomedicine has been recognized early,[6−9] and they represent the key building blocks of molecular biomimetics. In this context, several intriguing peptides, each able to recognize a different surface, have been recently found.[6] Each of them will have peculiar recognition mechanisms that to date remain elusive. Among others, cysteine-free gold-binding peptides (GBPs)[9−14] are particularly puzzling. Different GBPs have different origins[10−14] and are thus unrelated. Yet, the richness in hydroxy amino acids (HAAs), such as serine (Ser) and threonine (Thr), is a recurring and unexplained feature in GBPs. Motivated by this observation, we chose to focus on the role of HAAs and their hydration shell, by investigating how a prototype secondary structure (a solvated single antiparallel β-sheet) containing HAAs (Ser) interacts with Au. Using atomistic first-principle simulations, we show that weak interactions of dative-bond character confer to the amino acids in the β-sheet and its hydration layer the capability of discriminating among gold surface sites, thus fostering protein−gold recognition. Our simulation also highlights the role of hydration water in the gold-binding process, suggesting that hydrophilic proteins and their hydration shell cooperate to achieve surface site discrimination. Although our prototype cannot itself be classified as a GBP (these have more complex sequences than homoserine), HAAs in hydroxyl-rich GBPs have been suggested to be in contact with the gold surface,[15−17] and therefore the mechanism that we microscopically characterize may intervene in gold recognition by these GBPs as well. Clarifying the interactions of HAAs with gold is a crucial step to be performed before considering possible cooperative effects between the various amino acids composing a given GBP.

[†] CNR-Istituto di Nanoscienze.
[‡] Present address: Democritos Simulation Center, CNR-IOM Istituto Officina dei Materiali, Trieste, Italy.
[§] Politecnico of Torino.
[⊥] CNR-IMEM Institute of Materials for Electronics and Magnetisms.
[△] CINECA, Interuniversity Computing Center.

(1) Addadi, L.; Weiner, S. *Angew. Chem., Int. Ed. Engl.* **1992**, *31*, 153.
(2) Gray, J. J. *Curr. Opin. Struct. Biol.* **2004**, *14*, 110.
(3) Brown, S. *Proc. Natl. Acad. Sci. U.S.A.* **1992**, *89*, 8651.
(4) Perl-Treves, D.; Kessler, N.; Izhaky, D.; Addadi, L. *Chem. Biol.* **1996**, *3*, 567.
(5) Whaley, S. R.; English, D. S.; Hu, E. L.; Barbara, P. F.; Belcher, A. M. *Nature* **2000**, *405*, 665.
(6) Sarikaya, M.; Tamerler, C.; Jen, A. K.-Y.; Schulten, K.; Baneyx, F. *Nat. Mater.* **2003**, *3*, 577.
(7) Artzy-Schnirmann, A.; Zahavi, E.; Yeger, H.; Rosenfield, R.; Benhar, I.; Reiter, Y.; Sivan, U. *Nano Lett.* **2006**, *6*, 1870.
(8) Kacar, T.; Ray, J.; Gungormus, M.; Oren, E. E.; Tamerler, C.; Sarikaya, M. *Adv. Mater.* **2009**, *21*, 295.
(9) Nam, K. T.; Kim, D.-W.; Yoo, P. J.; Chiang, C.-Y.; Meethong, N.; Hammond, P. T.; Chiang, Y.-M.; Belcher, A. M. *Science* **2006**, *312*, 885.
(10) Huang, Y.; Chiang, C.-Y.; Lee, S. K.; Gao, Y.; Hu, E. L.; De Yoreo, J.; Belcher, A. M. *Nano Lett.* **2005**, *5*, 1429.
(11) Brown, S. *Nat. Biotechnol.* **1997**, *15*, 269.
(12) Tamerler, C.; Duman, M.; Oren, E. E.; Gungormus, M.; Xiong, X.; Kacar, T.; Parviz, B. A.; Sarikaya, M. *Small* **2007**, *2*, 1372.
(13) Kulp, J. L.; Sarikaya, M.; Evans, J. S. *J. Mater. Chem.* **2004**, *14*, 2325.
(14) Hnilova, M.; Oren, E. E.; Seker, U. O.; Wilson, B. R.; Collino, S.; Evans, J. S.; Tamerler, C.; Sarikaya, M. *Langmuir* **2008**, *24*, 12440.
(15) Braun, R.; Sarikaya, M.; Schulten, K. *J. Biomat. Sci.* **2002**, *13*, 747.
(16) Vila Verde, A.; Acres, J. M.; Maranas, J. K. *Biomacromolecules* **2009**, *10*, 2118.
(17) So, C. R.; Kulp, J. L., III; Oren, E. E.; Zareie, H.; Tamerler, C.; Evans, J. S.; Sarikaya, M. *ACS Nano* **2009**, *3*, 1525.

 10.1021/ja909823n

Computational methods can, in general, help shed light on the intimate nature of the protein−surface interface.[18,19] Classical molecular dynamics (MD), based on empirical force fields, has been used to study the interaction of peptides and proteins with gold surfaces.[15,16,20−23] Some works specifically focused on GBPs. Braun et al.[15] investigated the interaction of a GBP[11−13] with the Au(111) and Au(211) surfaces, finding differences in interaction energies and in the water population at the peptide−surface interface. Recently, Heinz et al.[22] studied different binding peptides on Au(111), Au(100), Pt(111), and mixed Au/Pt surfaces using a force field that reproduces the hydrophilicity of the Au surfaces.[23] Vila Verde et al.[16] compared a GBP[11] and a non-GBP on Au(111) by using a force field also tuned to reproduce gold hydrophilicity. They suggested that the higher flexibility of the GBP with respect to the non-GBP made less unfavorable the conformation rearrangements needed to increase the direct peptide−surface contact. Classical force fields have been also used to study the interaction of proteins with inorganic surfaces other than gold, including platinum,[24] rutile,[25,26] magnesium oxide,[27] hydroxyapatite,[28] silicon,[29] graphite,[30,31] carbon nanotubes,[32] diamond,[33] and self-assembled monolayers on inorganic surfaces.[34]

To date, quantum mechanical calculations at the density functional theory (DFT) level were applied only to study minimum energy structures (i.e., no molecular dynamics) of single amino acids on the gold surface and neglecting solvent effects.[35−40] The chemisorption of Cys on Au(111) has been investigated by Di Felice and Selloni[35] and by Nazmutdinov et al.[36] Ghiringhelli and Delle Site[37] studied the conformational changes for Phe adsorbed on different metal surfaces (Cu(111), Ag(111), and Au(111)). Hong et al.[38] investigated interaction strengths and adsorption geometries for six natural amino acids (Asp, Lys, Arg, Ser, Pro, Val) on Au(111) and a Au(111)/(111) ridge in vacuo or coadsorbed with a few water molecules. In the framework of developing a force field for protein−Au(111) interactions, our group has studied the interaction of 14 small molecules (representative of the natural amino acid functional groups) with a slab of Au(111) in the DFT periodic supercell approach.[39,40]

In the present work, we present the first ab initio molecular dynamics (AIMD) simulation of the interaction between a prototype protein and an inorganic surface, which also includes explicitly the solvent (water). AIMD, based on DFT, requires no empirical parameters, at odds with classical MD, and thus allows for an unbiased description of the interface. Moreover, AIMD gives direct access to the electronic structure of the system, i.e., to the microscopic origin of the interactions between gold, the protein, and the solvent. At difference with previous DFT calculations, AIMD simulations are not confined to the search of a global (or a few local) minimal energy structure, but can explore the dynamical behavior of the system. Concerning the current limitations of AIMD, we note the rather limited system sizes and simulation times that can be practically afforded with respect to classical MD and the accuracy of the AIMD-available DFT functionals (see Materials and Methods). Despite these limitations, we show here that this technique gains more insight on the nature and mechanisms of peptide/surface coupling with respect to previous knowledge, especially in terms of charge distribution, adding to previous findings on similar systems.

Materials and Methods

The choice to arrange the Ser amino acids as a β-sheet was suggested by the known importance of this conformation for the interaction with surfaces.[41] Certain surfaces may even induce the β-sheet structure.[42] Moreover, the β-sheet is also computationally convenient to simultaneously study multiple amino acids interacting with the surface due to its planarity. The relevance of the β-sheet conformation for the GBPs that have been discovered so far is uncertain. In fact, conformation of GBPs are largely unknown: in a few cases GBPs in water have been investigated by NMR and circular dichroism, showing disordered systems with little secondary structure elements.[13,14,17] As for the structure of GBPs when adsorbed on the surface, experimental evidence is even more scarce, and no direct structural data are available.

The Ser β-sheet of our simulation lies on a gold slab and is fully solvated with water (Figure 1).

Periodic boundary conditions are used in all three dimensions. A few water molecules, called *interstitial* in the following, are present also between gold and the β-sheet (Figure 1c). We distinguish between two inequivalent protein/water interfaces (gray boxes in Figure 1a), one in contact with the gold surface (interface 1) and the other facing liquid water (interface 2). The evolution of the system is simulated for 20 ps, a duration that is at the forefront for AIMD of systems as complex as ours and enables meaningful statistics. The sampling quality is further improved by the large numbers of water molecules (114), gold atoms (112), and amino acids (12).

We carried out ab initio molecular dynamics simulations in the canonical ensemble, using the Car−Parrinello algorithm[43] implemented in the quantum-espresso package (Giannozzi, P.; et al. http:\\www.quantum-espresso.org).[44] The electronic struc-

(18) Harding, J. H.; Duffy, D. M.; Sushko, M. L.; Rodger, P. M.; Quigley, D.; Elliot, J. A. *Chem. Rev.* **2008**, *108*, 4823.
(19) Cohavi, O.; Corni, S.; De Rienzo, F.; Di Felice, R.; Gottschalk, K. E.; Hoefling, M.; Kokh, D.; Molinari, E.; Schreiber, G.; Vaskevich, A.; Wade, R. C. *J. Mol. Rec.* DOI: 10.1002/jmr.993.
(20) Bizzarri, A. R.; Costantini, G.; Cannistraro, S. *Biophys. Chem.* **2003**, *106*, 111.
(21) Setty-Venkat, A.; Corni, S.; Di Felice, R. *Small* **2007**, *8*, 1431.
(22) Heinz, H.; Farmer, B. L.; Pandey, R. B.; Slocik, J. M.; Patnaik, S. S.; Pachter, R.; Naik, R. R. *J. Am. Chem. Soc.* **2009**, *131*, 9704.
(23) Heinz, H.; Vaia, R. A.; Farmer, B. L.; Naik, R. R. *J. Phys. Chem. C* **2008**, *112*, 17281.
(24) Ghiringhelli, L. M.; Hess, B.; van der Vegt, N. F. A.; Delle Site, L. *J. Am. Chem. Soc.* **2008**, *130*, 13460.
(25) Monti, S. *J. Phys. Chem. C* **2007**, *111*, 16962.
(26) Skelton, A. A.; Liang, T.; Walsh, T. R. *ACS Appl. Mater. Interfaces* **2009**, *1*, 1482.
(27) Cormack, A. N.; Jess Lewis, R.; Goldstein, A. H. *J. Phys. Chem. B* **2004**, *108*, 20408.
(28) Makrodimitris, K.; Masica, D. L.; Kim, E. T.; Gray, J. J. *J. Am. Chem. Soc.* **2007**, *129*, 13713.
(29) Cole, D. J.; Payne, M. C.; Colombi Ciacchi, L. *Phys. Chem. Chem. Phys.* **2009**, *11*, 11395.
(30) Raffaini, G.; Ganazzoli, F. *Langmuir* **2003**, *19*, 3403.
(31) Tomasio, S. M.; Walsh, T. R. *J. Phys. Chem. C* **2009**, *113*, 8778.
(32) Tomasio, S. M.; Walsh, T. R. *Mol. Phys.* **2007**, *105*, 221.
(33) Horinek, D.; Serr, A.; Geisler, M.; Pirzer, T.; Slotta, U.; Lud, S. Q.; Garrido, J. A.; Scheibel, T.; Netz, R. R.; Hugel, T. *Proc. Natl. Acad. Sci. U.S.A.* **2008**, *105*, 2842.
(34) Latour, R. A. *Biointerphases* **2008**, *3*, FC2.
(35) Di Felice, R.; Selloni, A. *J. Chem. Phys.* **2006**, *120*, 4906.
(36) Nazmutdinov, R. R.; Zhang, J. D.; Zinkicheva, T. T.; Manyurov, I. R.; Ulstrup, J. *Langmuir* **2006**, *22*, 7556.
(37) Ghiringhelli, L. M.; Delle Site, L. *J. Am. Chem. Soc.* **2008**, *130*, 2634.
(38) Hong, G.; Heinz, H.; Naik, R. R.; Farmer, B. L.; Pachter, R. *ACS Appl. Mater. Interfaces* **2009**, *1*, 388.
(39) Iori, F.; Di Felice, R.; Molinari, E.; Corni, S. *J. Comput. Chem.* **2009**, *30*, 1465.
(40) Iori, F.; Corni, S.; Di Felice, R. *J. Phys. Chem. C* **2008**, *112*, 13540.
(41) Graether, S. P.; Kuiper, M. J.; Gagné, S. M.; Walker, V. K.; Jia, Z.; Sykes, B. D.; Davies, P. L. *Nature* **2000**, *406*, 325.
(42) Kowalewski, T.; Holtzman, D. M. *Proc. Acad. Sci. U.S.A.* **1999**, *96*, 3688.
(43) Car, R.; Parrinello, M. *Phys. Rev. Lett.* **1985**, *55*, 2471.
(44) Giannozzi, P.; et al. *J. Phys.: Condens. Matter* **2009**, *21*, 395502.

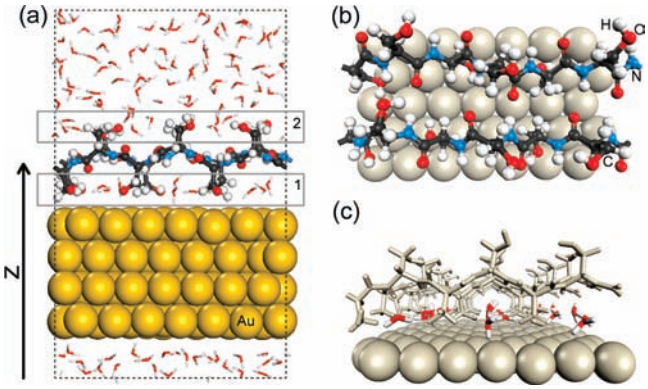

Figure 1. (a) Side view of the system in the simulated unit cell (dashed line). Gray boxes (labeled 1 and 2) identify 2 Å thick regions that include the two different protein−water interfaces referenced in the text. (b) Top view of the periodically repeated β-sheet unit on the gold surface. The unit cell contains 12 Ser residues, arranged in two β-strands. (c) Side view of the simulated system where the nine interstitial water molecules are spotted. These are uniformly distributed in the three grooves that result from the $-CH_2OH$ Ser side chains and the surface. The simulation cell is repeated along the groove direction. Gray spheres represent Au atoms in (b) and (c).

ture was calculated in the DFT framework, and the PBE generalized gradient approximation[45] was applied to the exchange−correlation functional. Electron−ion interactions were treated with ultrasoft pseudopotentials of the Vanderbilt type.[46] The single-particle wave functions (charge density) were expanded in plane waves up to a kinetic energy cutoff of 25 Ry (200 Ry). The semicore 5d electrons of Au were explicitly included in the valence shell. These pseudopotentials and the related cutoffs have been preliminary tested and yielded reliable results in previous applications.[40,46] The simulations were performed at the Γ point of the supercell Brillouin zone (BZ).

A periodically repeated supercell with the size $10.159 \times 20.529 \times 32.656$ Å^3 was used. The system (586 atoms, 2552 electrons) is composed of a four-layer slab of Au(111) with $2\sqrt{3} \times 7$ lateral periodicity and two antiparallel strands of polyserine (six amino acids per strand) to form a two-dimensional (2D) periodic β-sheet. The choice of this anisotropic cell enables a good matching between surface and β-sheet in-plane periodicity. The interface is topped by 105 water molecules that simulate a 15 Å thick region of liquid water, with a density of 1.1 g/cm^3 at room temperature. Negligible finite size effects were found for AIMD simulations of liquid water in a cubic cell with size of approximately 11 Å,[47] i.e., comparable to the smallest dimension of the supercell employed here.

The deuterium mass was assigned to hydrogen nuclei, to allow for a larger time step. In the molecular dynamics calculation the fictitious mass associated with the plane waves coefficients was set to 450 au, which allowed for a time step of 0.17 fs in the numerical integration of the equations of motion. This set of values was previously tested also on the separate liquid water and surface gold subsystems, giving dynamical properties in good agreement with previous AIMD results.[47−49] The ionic temperature was controlled by coupling the nuclei to a chain of two Nosé−Hoover thermostats with frequencies $\omega_1 = 30$ THz and $\omega_2 = 15$ THz, respectively, in order to activate both the soft modes of the Au surface and the stiff modes of protein and water at the same time. The average temperature of the system was set to 400 K, that is, the temperature that seems to better simulate the structural properties of water at room temperature.[47,49] Small-gap and, in particular, metallic systems suffer from undesired heat transfer from the ionic to the fictitious electronic degrees of freedom during finite-temperature Car−Parrinello propagation.[50] To fix this problem, we coupled a further Nosé−Hoover thermostat ($\omega_e = 200$ THz) to the electronic orbital degrees of freedom in the Car−Parrinello Lagrangian.

The initial configuration was obtained from classical molecular dynamics. Briefly, classical simulations were run on large, non fully periodic β-sheets on rigid Au(111) for tens of nanoseconds to equilibrate water in the protein−surface interstice. The system used for AIMD was extracted from the end point of these simulations and was further equilibrated for hundreds of picoseconds. The final coordinates of this equilibration were used as the starting point for AIMD. More details on the entire setup procedure are given in the Supporting Information.

The AIMD simulation was carried out for 20 ps, the first 7 ps of which were used to thermalize the system at 400 K: this equilibration phase was discarded in the statistical analysis. The ionic and electronic thermostats were activated during the entire simulation in order to avoid drifts in the fictitious electronic kinetic energy and in the Lagrangian constant of motion. The long (for standard AIMD) production time of 13 ps, along with the redundancy of the prepared system, yields a fair statistical analysis of the results.

The evolution of the electronic structure of the system was followed by sampling the trajectory every $\delta t = 0.5$ ps. For each selected configuration we performed single-point DFT calculations, using the PWscf code, also included in the quantum-espresso suite. Computational details (e.g., energy cutoffs, pseudopotentials, XC functionals) are the same as in the CP simulation, but the BZ sampling was performed over 12 special **k**-points in the irreducible wedge of the 2D BZ.

A possible concern regarding the applied methodology is the well-known deficiency of present GGA functionals to account for long-range dispersion interactions.[51] In principle, this might have consequences on the interaction of the protein both with water and with the surface. As we discuss in more detail in the Supporting Information, on the basis of the known performance of PBE (which reproduces reasonably well hydrogen bonds)[52] and of existing tests available in the literature,[53−56] none of the conclusions presented here should be affected by the missing dispersion interactions (although other quantities that we do not discuss, such as interaction energies, could indeed be modified).

Results and Discussion

We initially examine how the β-sheet interacts with the surface, within the simulation time. To this aim, we analyze the amount of charge transfer between the Ser side chains and gold, as well as any indication of hybridization between the orbitals of the β-sheet and the gold surface. The direct access to the system electronic properties is possible only because of the first-principle character of the dynamics.

Although we do not recognize the formation of any covalent bond between the β-sheet (or water) and the surface, a weak but not negligible electronic interaction exists, beyond the simple physisorption picture. This weak-interaction regime can be described as an incipient oxygen-to-gold dative bond, and it is not related to nonbonding interactions (e.g., van der Waals

(45) Perdew, J. P.; Burke, K.; Ernzerhof, M. *Phys. Rev. Lett.* **1996**, *77*, 3865.
(46) Vanderbilt, D. *Phys. Rev. B* **1990**, *41*, R7892.
(47) Sit, P.H.-L.; Marzari, N. *J. Chem. Phys.* **2005**, *122*, 204510.
(48) Silvestrelli, P. L.; Parrinello, M. *J. Chem. Phys.* **1999**, *111*, 3572.
(49) Grossman, J. C.; Schwegler, E. S.; Draeger, E. W.; Gygi, F.; Galli, G. *J. Chem. Phys.* **2004**, *120*, 300.
(50) Pastore, G.; Smargiassi, E.; Buda, F. *Phys. Rev. A* **1991**, *44*, 6334.
(51) Kohn, W.; Meir, Y.; Makarov, D. E. *Phys. Rev. Lett.* **1998**, *80*, 4153.
(52) Zhao, Y.; Truhlar, D. *J. Chem. Theory Comput.* **2005**, *1*, 415.
(53) Lazić, P.; Crljen, Z.; Brako, R.; Gumhalter, G. *Phys. Rev. B* **2005**, *72*, 245407.
(54) Ferretti, A.; Baldacchini, C.; Calzolari, A.; Di Felice, R.; Ruini, A.; Molinari, E.; Betti, M. G. *Phys. Rev. Lett.* **2007**, *99*, 046802.
(55) Wippermann, S.; Schmidt, W. G. *Phys. Rev. B* **2008**, *78*, 235439.
(56) Langreth, D. C.; et al. *J. Phys.: Condens. Matter* **2009**, *21*, 084203.
(57) Löwdin, P.-O. *Adv. Quantum Chem.* **1970**, *5*, 185.

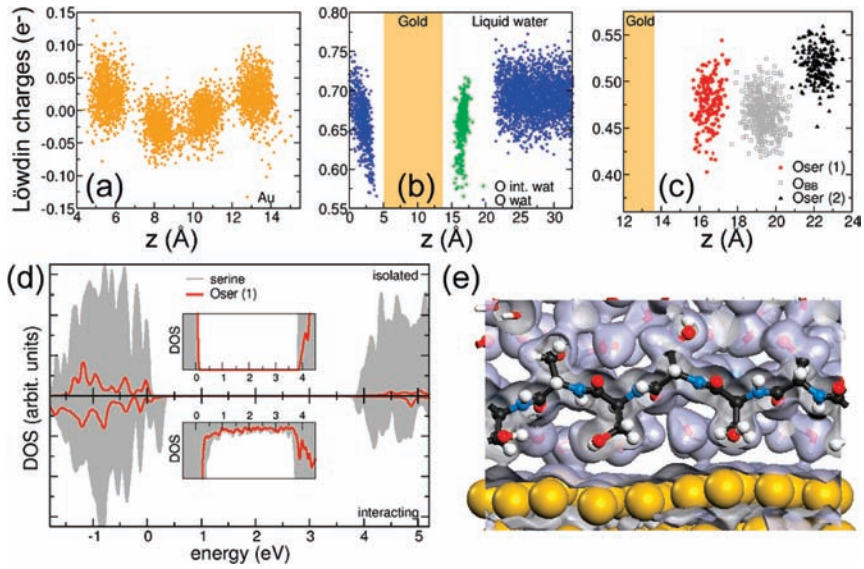

Figure 2. (a−c) Distributions of the Löwdin net atomic charges for selected atoms along the direction normal to the surface, obtained by sampling the electronic structure every 0.5 ps during the AIMD simulation. (a) Charge distribution for the four Au layers. (b) Atomic charges of interstitial (green) and liquid (blue) water oxygens. (c) Atomic charges of oxygens of Ser side chains (O_{ser}), at interface 1 (red dots) and 2 (black triangles). Charges of the backbone oxygens, O_{BB}, are also reported (gray squares). (d) DOS projected on the protein (gray area) in the gas phase (upper panel) and in the interacting configuration (lower panel), i.e., including Au and water. The DOS is computed for a representative snapshot of the trajectory. The red line is the DOS projection on the O_{ser} atoms of interface 1. DOS are collected aligning the lowest single-particle eigenvalues. The zero-energy reference is set to the HOMO of the isolated molecule. Insets enlarge the HOMO−LUMO gap area. (e) Isosurface plot of the total charge density at the surface region, same snapshot as in panel (d).

forces). Figure 2a−c shows the distribution of Löwdin net atomic charges[57] during the simulation for gold and oxygen atoms of water (O_{wat}) and Ser side chains (O_{ser}). The Löwdin population analysis reveals a small, but evident, electron donation from the Ser hydroxyl groups and water molecules to the gold surface. Gold atoms of the inner zone (Figure 2a) maintain an average neutral behavior (i.e., $q \sim 0e^-$), whereas those of the two external layers present a net electron accumulation. The opposite is true for water molecules close to the surface (Figure 2b) and for the O_{ser} belonging to interface 1 (Figure 2c), which roughly donate an average charge amount of $\sim 0.05e^-$ per oxygen atom. Water molecules distant, >3−4 Å, from the surface and the O_{ser} of the interface **2** are instead hardly affected by the presence of the metal.

In principle the charge shifts may also be due to substantial polarization effects (which would similarly provide a significant stabilization) instead of dative bonding. However, Figure 2d explicitly reveals the orbital hybridization that takes place at the interface, considering the modification in the density of states (DOS) of Ser in the gas phase ("isolated") and in the presence of water and gold ("interacting"). The isolated configuration (upper panel) has a sharp HOMO−LUMO gap, typical of the molecular system. When the molecule is immersed in solution and in contact with the surface, its density of states is changed and the gap is reduced (see insets): a non-negligible DOS for the interacting molecule is present in the pristine gap region, which is related to charge transfer to the gold surface. Similar is the case of interstitial water, as shown in Figure 2e, where the total electronic charge for a representative snapshot of the dynamics is reported (see also Figure S1): the presence of charge density spread between interstitial water molecules and the surface is an indication of an orbital hybridization at the interface.

These results disclose the intimate nature of the interaction between hydroxyl amino acids and gold in a complex environment, where solvation water is also present. In particular, *we conclude that a weak surface/side-chain interaction is active, but no strong chemisorption exists for the polyserine on Au(111)*, in agreement with experimental estimates of the affinity of Ser homopeptides for gold.[58,59]

The picture that we elicit from the above findings is that, despite the fact that the binding at any surface site is weak, several such weak side-chain/surface interactions may sum up to give rise to substantial binding. This binding is also selective when (i) the protein is capable of *surface-site discrimination*, i.e., the side chains in contact with the surface prefer to stay on one specific adsorption site among all the available sites, and (ii) the protein is structurally rigid[7] and the arrangement of the side chains matches the most favorable interaction sites on the surface.[17,60]

The arrangement of side chains, as well as the rigidity, depends on the sequence and the structure of the precise peptide under study. Therefore, since our prototype system is not a GBP, it is beyond the scope of the present article to verify whether a mechanism based on surface-site discrimination plus site-matching is ruling the specificity of any of the GBPs identified so far. Nevertheless, condition (i), i.e., surface-site discrimination, is hard-coded in the interaction between the hydrated side chains and the surface, and we can verify if, in the case of Ser, such interaction leads to clear surface-site discrimination or not. We thus investigate whether the incipient dative bonding between the β-sheet and the surface leads to clear adsorption site preferences and what these preferences are. To avoid trapping of the hydrated β-sheet in an ordered local energy minimum, matching between the arrangement of O_{ser} atoms and the Au lattice inside the unit cell is deliberately inhibited by construction. The β-sheet is thus free to explore multiple

(58) Willett, R. L.; Baldwin, K. W.; West, K. W.; Pfeiffer, L. N. *Proc. Natl. Acad. Sci. U.S.A.* **2005**, *102*, 7817.
(59) Peelle, B. R.; Krauland, E. M.; Wittrup, K. D.; Belcher, A. M. *Langmuir* **2005**, *21*, 6929.
(60) Oren, E. E.; Tamerler, C.; Sarykaya, M. *Nano Lett.* **2005**, *5*, 415.

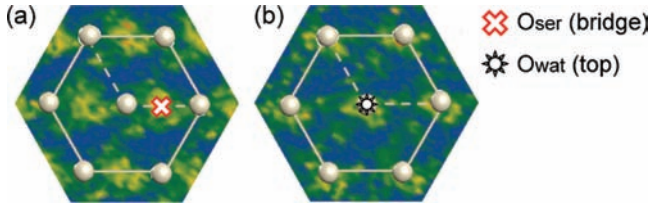

Figure 3. (a) g_{AuOser} and (b) g_{AuOwat}, calculated with respect to the Au atoms of the topmost plane. Color scale: blue = no density, red = max density. The symbols highlight the adsorption site preferences for O_{ser} and O_{wat} with respect to the Au(111) surface lattice, as resulting from the maxima of g_{AuO}. Spheres represent the Au lattice.

adsorption sites during the simulation. The attempt of the hydrated protein to dynamically select the most favorable configuration at each time step is proof that the protein is able to sense the atomic arrangement of the gold surface, as revealed by analyzing *statistically* preferred adsorption sites.

To shed light on this issue, we present in Figure 3 the two-dimensional Au−O in-plane distribution functions $g_{AuO}(x,y)$ (see also Supporting Information) for the O_{ser} atoms in contact with the surface and for the O_{wat} atoms of the insterstitial water molecules, g_{AuOser} and g_{AuOwat}, respectively. $g_{AuO}(x,y)$ represents the density of oxygen atoms as a function of the in-plane coordinates x,y relative to a given gold atom, averaged on all the surface gold atoms, and it is defined in the Supporting Information.

g_{AuOser} in Figure 3a shows a clear structuring of the Ser oxygens around Au atoms. In particular, O_{ser} atoms prefer to reside at some of the available bridge sites, statistically forming one-dimensional motifs along one of the two substrate lattice directions. Bridge sites are themselves a subset of all the possible adsorption sites at the surface, which include also top and 3-fold fcc locations. Therefore, the β-sheet is indeed selecting some adsorption sites over others. This is an important result: *a hydroxyl-rich protein is capable of discriminating between gold surface sites.* Surface-site preference of adsorbed peptides was previously reported on the basis of classical MD simulations,[22] with the introduction of the concept of soft epitaxy. While our ab initio analysis confirms the existence of adsorption at specific sites rather than spread on the surface, we find adsorption sites different from those of adsorbed molecules in classical MD,[22] namely, *bridge* instead of *fcc*. Establishing the preferred adsorption site has important practical consequences, because a possible strategy to design surface-specific proteins is to arrange side-chain positions to match preferred adsorption sites.

The hydroxyl groups of Ser are not the only species that interact with the surface: the charge transfer analysis in Figure 2 reveals a water−Au interaction as well. By further inspection, we show that the recognition also occurs through the water molecules of the first hydration shell. The OH groups of Ser create a close-to-planar layer; a regular pattern of O_{ser} atoms is thus exposed to the inorganic surface.

The atomic density profile in the direction perpendicular to the surface (Figure 4a) reveals that water creates a hydration layer that superimposes to this O_{ser} layer, both for the gold/protein (**1**) and for the protein/water (**2**) interfaces. Water molecules intercalate among Ser hydroxyls and are H-bonded to them and to each other.

Therefore, we conceive the protein boundary as a complex entity defined by the Ser hydroxyl groups and the intercalating water molecules. To be relevant for recognition, these water molecules should also occupy well-defined positions on the protein boundary. To inquire on this behavior, we inspect the atomic density map of hydration water oxygens in interfaces 1 and 2 (Figure 4b). The results for interface 1 are reported in the left panel of Figure 4b: the nine high-density spots (red), separated by regions of negligible density (blue), correspond to the nine O_{wat} atoms of interstitial water molecules.

The six exposed O_{ser} atoms produce an atomic density map (Figure 5) with high-density spots that are virtually indistinguishable from those of O_{wat} in Figure 4b. We conclude that hydration water molecules occupy precise positions on the protein surface, similarly to O_{ser}. This structuring is not induced by gold, because similar sharp spots are present in the protein/water interface **2** as well (Figure 4b, right panel). Moreover, the sharpness of the hydration water structure is not an artifact related to the investigated time scale. We observe that hydration water molecules do exchange between the localized sites in the protein surface and with the liquid water layer,[61] but they spend little time in regions outside the density maxima. Structuring of the hydration water has also been reported for the threonine β-sheet of an antifreeze protein.[62]

Next, we consider the interactions of interstitial water with the surface, searching for surface-site discrimination as done for Ser. g_{AuOwat} in Figure 3b, calculated for the interstitial water molecules in contact with the surface, shows that O_{wat} prefer on-top locations. The resulting pattern represents a genuine

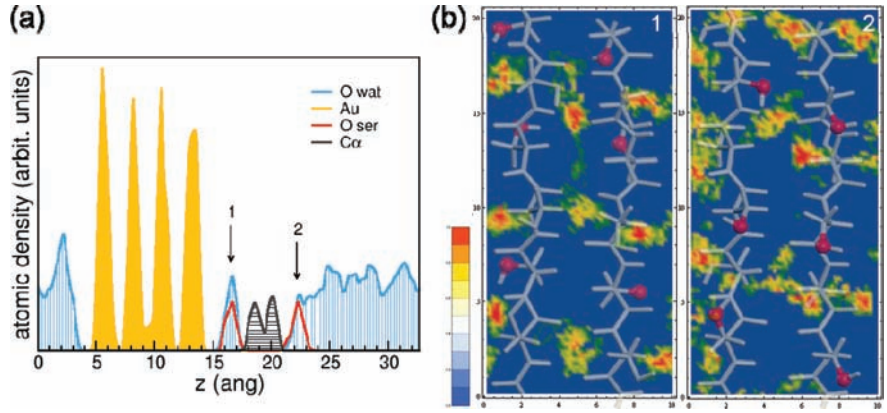

Figure 4. (a) Atomic density profile along the surface normal. Vertical arrows identify interfaces 1 and 2 of Figure 1. (b) Water molecule distribution at the interfaces 1 (left) and 2 (right), parallel to the surface. Two-dimensional atomic density maps are calculated collecting the positions of the O_{wat} atoms, with respect to the protein position. The collective translational displacements of the protein are removed. Color code is the same as that in Figure 3, in log scale. The atomic structure of the protein is superimposed for clarity (gray sticks). Hydroxyl O_{ser} atoms are marked with red spheres.

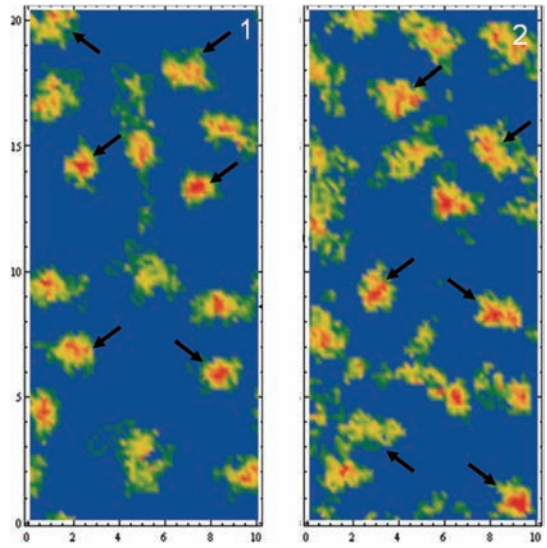

Figure 5. Two-dimensional atomic density maps of O_{wat} + O_{ser} atoms within the interfaces 1 and 2 defined in Figure 1. The collective translational displacements of the protein are removed. Color code: blue = no density, red = max density, in a logarithmic scale (the same as Figure 4). The spots indicated by arrows represent the density maxima due to the Ser side-chain oxygens (O_{ser}). Note the similarity in sharpness, shape, and size between these spots and those due to O_{wat}, namely, those not indicated by arrows.

adsorption preference of hydration water, which is identical at the other water/gold interface (not shown). This outcome demonstrates that *the hydration layer*, i.e., the shell of water molecules tightly bound to the β-sheet, *plays an active role in surface-site discrimination by the peptide, via its own adsorption site preferences*. The importance of the interaction strength of the solvent and its complementarity with the metal surface, as well as other solvation effects, was previously noted.[22] Our results focus instead on the specific role of the β-sheet hydration layer and support the concept of the hydrated protein as a single entity, where both the protein and the hydration layer contribute to the recognition process, competing with the rest of the solvent for the gold surface.

In particular, hydration water molecules and the Ser side chains act in a cooperative way to bind the protein to specific sites on the gold surface. The O_{wat} atoms of interstitial water molecules, which benefit from a higher flexibility than Ser side chains, first occupy the most favorable adsorption sites, namely, the top sites.[64] The protein consequently arranges on the second best adsorption sites (bridge) in order to optimize the interaction with the surface while maintaining hydrogen bonds with the on-top water molecules. This synergic behavior favors an interaction as large as possible and thus an effective adhesion of the protein on the surface. Remarkably, g_{AuOser} and g_{AuOwat} in Figure 3 are genuine results of the ab initio simulation, not reminiscent of the initial structure of the dynamics, as discussed in the Supporting Information. It is also to be noted that empirical force fields using Lennard-Jones potentials centered on Au atoms[23] lead to preferential adsorption of polarizable groups such as O_{ser} in the fcc site.[22] The tendency of atom-centered LJ potentials to yield adsorption of single molecules in a high-coordination site (such as fcc) was noted before (e.g., ref 63 for single water molecules), at odds with the present ab initio results and previous static DFT investigations on water[39,64] and compounds analogous to the Ser side chain (methanol[39,65] and ethanol[66]) on Au(111). We remark that in principle the adsorption site preferences of water molecules in the liquid depend not only on the single molecule preferences but also on their complex interplay with the H-bond network.

Conclusions

In summary, we have identified the fundamental nature of the interaction between a gold surface and a solvated β-sheet composed of HAAs (that are frequently found in experimental GBPs). In particular, we find that an electronic interaction with an incipient dative bond character confers to Ser and water the capability to discriminate between gold surface sites. Although GBPs will have richer and diverse gold recognition mechanisms, these findings disclose the potential role of Ser and other HAAs. Moreover, a picture where hydration water and peptide side chains cooperate to achieve surface recognition emerges from our simulation. As a whole, our study corroborates the use of ab initio methods for complex systems. For protein/surface interfaces, our AIMD simulation provides reliable adsorption site information, which is needed also for accurate force-field parametrizations. The latter would allow for classical simulations of large-scale hybrid systems on a quantum mechanical basis.

Acknowledgment. The EU FP6 project DEISA (DECI project PSI-Wat) is acknowledged for the computational time (350 000 CPU hours) on the supercomputer Mare Nostrum located at the Barcelona Supercomputer Centre. The work was funded by the EU through project Prosurf (contract FP6-NEST-028331).

Supporting Information Available: Further details on methods and system setup; definition and calculation of g_{AuO}; figure of charge density; comparison of g_{AuO} as found in the ab initio and the preparatory classical MD; tests on g_{AuO} convergence; discussion of dispersion interaction effects; complete refs 44 and 56. This material is available free of charge via the Internet at http://pubs.acs.org.

JA909823N

(61) Pizzuti, F.; Marchi, M.; Sterpone, F.; Rossky, P. J. *J. Phys. Chem. B* **2007**, *111*, 7584.
(62) Nutt, D. R.; Smith, J. C. *J. Am. Chem. Soc.* **2008**, *130*, 13066.
(63) Siepmann, J. I.; Sprik, M. *J. Chem. Phys.* **1995**, *102*, 511.
(64) Michaelides, A.; Ranea, V. A.; de Andres, P. L.; King, D. A. *Phys. Rev. Lett.* **2003**, *90*, 216102.
(65) Chen, W.-K.; Lu, S.-H.; Cao, M.-J.; Yan, Q.-G.; Lu, C.-H. *J. Mol. Struct.: THEOCHEM* **2006**, *770*, 87.
(66) Fartaria, R. P. S.; Freitas, F. F. M.; Fernandes, F. M. S. S. *Int. J. Quantum Chem.* **2007**, *107*, 2169.